

PROPHECY OF INDOLIZINE CONTAINING C200-3231 USING MOLECULAR DYNAMIC SIMULATIONS & MACHINE LEARNING METHODS AGAINST CHRONIC MYELOID LEUKEMIA DISEASE

Sangeeta Mahaur^{1*}, Sukirti Upadhyay² and Jitendra³

^{1*,2}Department of Pharmacy, School of Pharmaceutical Sciences, IFTM University, 244001, Moradabad, Uttar Pradesh, India.

³Department of Information Technology, Indian Institute of Information Technology Allahabad, 211015, Uttar Pradesh, India.

Article Received on
20 July 2022,

Revised on 10 August 2022,
Accepted on 30 August 2022

DOI: 10.20959/wjpr202212-25476

***Corresponding Author**

Sangeeta Mahaur

Department of Pharmacy,
School of Pharmaceutical
Sciences, IFTM University,
244001, Moradabad, Uttar
Pradesh, India.

ABSTRACT

An abnormal and expeditious facsimile of oncogene bcr-abl protein in the stem cells has been recognized as the foremost cause of Chronic Myeloid Leukemia. It has been renowned that tyrosine kinase jurisdiction of bcr-abl protein is a probable remedial target for the accomplishment of Chronic Myeloid Leukemia. The persistence of the contemporaneous revision of the target and furthestmost optimized hit complex stability was explored by molecular dynamics. machine learning-based computational predictive models based on molecular dynamics trajectories for training machine learning models still need to be explored. In the current analysis, parameters have been extricated from the molecular dynamics approaches of the C200-3231 complex to

train paradigm operate quantum chemical energies and forces for accuracy and efficiency, long-ranged interactions, quantum kinetics, transferability of coarse-grained models, the kinetics of coarse-grained models, transferable prediction of intensive properties, equivariant generative networks with parameter sharing, explainable artificial intelligence methods or Deep tensor neural network, schNet and VAMPnet. C200-3231 complex was docked using the glide unit of Schrodinger software, and rapid molecular dynamics simulations of 10 ns were achieved for the cunning of molecular dynamics parameters. This research recognized that molecular dynamics parameters could be excellently used for the description of the C200-3231 complex accompanied by lead optimization.

KEYWORDS: CML, Indolizine, Machine learning, Molecular dynamic simulations, Quantum mechanics/Molecular mechanics.

1. INTRODUCTION

Cancer is the escalation progression of cells that can reside in encompass situations of the body.^[1] Chronic Myeloid Leukemia (CML) is a Myeloproliferative syndrome recognized for instance hematopoietic stem cell syndrome occasioned through the expansion or redundant split of granulocytes cells and propagation influential a high rise of white blood cell and total fashionable addition to a spleen enlargement or splenomegaly.^[2,3] Chronic Myeloid Leukemia organizes 15% of mature Leukemia through nearby 4600 recently analyzed circumstances per annum that occurred in the United States.^[4] The preliminary segment of the syndrome devours nearby 4-6 years. Chronic Myeloid Leukaemia additional accumulation of juvenile myeloid cells to mature granulocytes in the bone marrow, peripheral blood and spleen.^[5] Here the number of objectives identify cancer but bcr-abl protein is a consequence in Chronic Myeloid Leukemia, Chronic Neutrophilic Leukemia, Chronic Eosinophilic Leukemia as well as Idiopathic Myelofibrosis, Polycythemia Vera, Thrombocythemia, Acute Myeloid Leukemia (AML), Lymphoblastic Leukemia (LBL) and Acute Lymphoblastic Leukemia (ALL).^[6,7,8] Chronic myeloid Leukaemia is the pathogenesis of hematopoietic stem cells the Philadelphia chromosomes 9 and 22 were revealed through Peter Nowell in 1960. The situation initiates a translocation of the tyrosine kinases, the ABL (Abelson) gene from chromosome 9 and the BCR breakpoint cluster region gene from chromosome 22.^[3,9] Here, molecular magnitudes of this translocation instance are the development of the reciprocal abl/bcr on chromosome 9 and a chimeric gene bcr/abl on chromosome 22.^[10] This translocation creates the oncogenic bcr-abl protein merging genetic material in hematopoietic stem cells which translates an anomalous protein through constitutive tyrosine kinases action in the ability for apoptosis gestures.^[11] The occurrence of bcr-abl protein using tyrosine kinase was observed in more than 90% of Chronic Myeloid Leukaemia patients.^[12] Therefore, tyrosine kinase is responsible foreshadow the progression of Chronic Myeloid Leukaemia Cells. The mutant Philadelphia chromosomes are optimizing replica in delightful tyrosine kinase inhibitors (TKIs) in the direct cause of the resistance.^[12] Tyrosine kinase inhibitors are fashionable from N-terminal segment residues for the structure-based controls and the C-terminal segment residues for DNA enthusiastic binding sites.^[13] The tyrosine kinase inhibitors amplified in phosphorylation of bcr-abl protein control of cell divisions and mitosis.^[14,12] The Nilotinib, Dasatinib, Imatinib and Bosutinib designed

a sequence of atoms to inhibit the tyrosine kinase activity of the protein. Nilotinib and Imatinib could impede the uncontrolled kinase activity of the protein and inverse the hematologic structures of Chronic Myeloid Leukaemia.^[1,15]

Molecular dynamics is a simulation technique through the computer which permitted tracing interaction for atoms in the assured time interval. The molecular dynamics skill is constructed going on Newton's law and classic mechanics law. Molecular dynamics is the expenditure equation of Newton's law and classical mechanics.^[16] Molecular dynamics is a technique to examine the exploring structure of solid, liquid and gas. The molecular dynamics technique is welfare to the interaction of hard domains. The molecular dynamics phase involves a computational study of rigorous dynamism for every atom a chemical system monitored by a fewer luxurious integration phase develops the locations of the atoms permitting the conventional rules of gesticulation. Dynamism fields precisely the total force of three modules.^[17]

1. Bonded dynamism - Bonded dynamism consists of integrations concerning small groups of fragments associated with one or more covalent bonds.^[17]
2. Vander Waals dynamism - Vander Waals dynamism consists of integrations concerning entirely pairs of fragments in the system.^[17]
3. Electrostatic dynamism – Electrostatic dynamism consists of interactions concerning entirely pairs of fragments and falls off deliberate through distance.^[17]

The structure-based virtual screening of the Indolizine library from different databases.^[18] Molecular dynamics simulations selected the best compound nominated based on docking score, binding energy, ligand-protein interactions and ADME for the bcr-abl protein.^[18] The extensive docked tactics on bcr-abl had been accomplished by exhausting simple precision and extra precision approach and discovering the best persuasive compounds appraised via absorption, distribution, metabolism and elimination factors.^[18,19] Further, the target and most optimized hit complex stability were investigated by Molecular Dynamics.

Machine learning in molecular simulations is precise on neural systems for the estimate of forces on coarse-grained molecular dynamics, quantum mechanical energies, extraction of free energy surfaces and kinetics and molecular equilibrium structures and computing thermodynamics.^[20] Machine learning models in molecular dynamic simulations are based on quantum mechanics and molecular mechanics have been developed to simulate molecular systems and description of changes in electronic structures that employ force field parameters

and high dimensional neural network potential.^[21] Deep learning presents specific methods and neural networks for molecular dynamic simulations.

1. Behler-Parrinello networks have predicted the molecular systems to run QM molecular dynamic simulations across a large chemical space.
2. Deep tensor neural networks and schNet algorithm learns to extract information in the bone structure of the chemical compound and configuration space to simulate molecular dynamics.^[21]
3. Coarse graining (CGnets) predicts a free energy surface that is quantitatively equivalent to the free energy surface of the entire atom simulations and regulates the identical metastable states.
4. VAMPnets is optimized by regression error in latent space and replace the complications of pharmacokinetics.
5. Markov state model is a precise estimation of the extensive time kinetics to create an effective distribution for small molecular dynamics benchmark systems.^[20]
6. Boltzmann generators predict performing linear interpolations in latent space.

Machine learning for molecular simulation predicts accuracy and efficiency in quantum chemical energies and forces, long-range interactions, quantum kinetics, transferability of coarse-grained models, the kinetics of coarse-grained models, transferable prediction of intensive properties, equivariant generative networks with parameter sharing, explainable artificial intelligence methods (Deep tensor neural network, schNet and VAMPnet).^[20,21]

1.1 POTENTIAL ENERGY OF THE SYSTEM

Born-Oppenheimer, time-independent wave function mechanics, the electronic energy including nuclear repulsion E_{QM} for the choice of the suitable model according to newton's second law.^[21,21]

$$\hat{H}_{QM}\psi_R(\vec{r}) = E_{QM}(\vec{R})\psi_R(\vec{r}) \quad (1)$$

$$\hat{H}_{QM} = -\frac{1}{2} \sum_i^{N_{el}} \nabla_i^2 + \sum_{i<j}^{N_{el}} \frac{1}{|\vec{r}_i - \vec{r}_j|} - \sum_i^{N_{el}} \sum_j^{N_{QM}} \frac{Z_j}{|\vec{r}_i - \vec{R}_j|} + \sum_{i<j}^{N_{QM}} \frac{Z_i Z_j}{|\vec{R}_i - \vec{R}_j|} \quad (2)$$

$$E_{QM}(\vec{R}) = \frac{\langle \psi(\vec{r}) | \hat{H}_{QM} \psi(\vec{r}) \rangle}{\langle \psi(\vec{r}) | \psi(\vec{r}) \rangle} \quad (3)$$

$$-\frac{\partial E_{QM}(\vec{R})}{\partial \vec{R}_i} = \vec{F}_i = m_i \frac{d\vec{v}_i}{dt} \quad (4)$$

In eq. (4) Where, E_{QM} = Electronic energy nuclear repulsion for eigen function (quantum Born- Oppenheimer approximated potential energy), \vec{R} = gradients of the nuclei, \vec{F}_i = force of particle i , m_i = mass, \vec{v}_i = velocity, t = time.

1.2 CLASSICAL FORCE FIELDS SYSTEM

The potential energy of the system is calculated with a force field for molecular dynamic simulations.^[20,21]

$$E_{MM}(\vec{R}) = E^{\text{bond}}(\vec{R}) + E^{\text{angle}}(\vec{R}) + E^{\text{dihedral}}(\vec{R}) + E^{\text{el}}(\vec{R}) + E^{\text{vdw}}(\vec{R}) \quad (5)$$

In eq. (5), Where, E^{bond} = contribution of all covalent bonds, E^{angle} = contribution of all covalent angles, E^{dihedral} = contribution of all covalent dihedral, E^{el} = electrostatic interactions, E^{vdw} = vander waals interactions.

1.3 QUANTUM MECHANICS/MOLECULAR MECHANICS (QM/MM) SCHEME

QM/MM is a hybrid approach that combines a QM subsystem with an MM environment in a balance between cost and accuracy.^[20,21]

$$E_{QM/MM}(\vec{R}) = E_{QM}(\vec{R}_{QM}) + E_{MM}(\vec{R}) - E_{MM}(\vec{R}_{QM}) \quad (6)$$

In eq. (6), Where, $E_{QM/MM}$ = energy of QM subsystem E_{QM} and energy of MM surrounding E_{MM} , $E_{QM}(\vec{R})$ = energy of the QM subsystem, $E_{MM}(\vec{R})$ = energy of the complete system calculated with the classical force field, $E_{MM}(\vec{R}_{QM})$ = energy of the QM zone calculated with the force field, \vec{R} = all nuclei in the system, \vec{R}_{QM} = nuclei treated quantum mechanically QM zone, \vec{R}_{MM} = atom treated classically MM zone.

1.4 MACHINE LEARNING OF POTENTIAL-ENERGY SURFACES

Machine learning method used high-dimensional neural network potentials (HDNNP_S) and (feed-forward neural networks, FNN_S). HDNNP_S is a powerful technique to learn the requirement for limited extrapolation capabilities, large training sets, and the danger of overfitting.^[20,21]

$$\Delta E(\vec{R}) = E^{\text{expression}}(\vec{R}) - E^{\text{cheap}}(\vec{R}) \quad (7)$$

1.5 THE ROOT MEANS SQUARE DEVIATION

RMSD is used to measure the average change in displacement of a selection of atoms for a particular frame concerning a reference frame. It is calculated for all frames in trajectory. The RMSD for frame x is:

$$\text{RMSD}_x = \sqrt{\frac{1}{N} \sum_{i=1}^N (r'_i(t_x) - r_i(t_{\text{ref}}))^2} \quad (8)$$

In eq. (8), Where N is the number of atoms in the selection, t_{ref} is the reference time, r' is the position of the selected atoms in frame x after superimposing on the reference frame, is frame x recorded time.

1.6 THE ROOT MEAN SQUARE FLUCTUATION

RMSF is useful for characterizing local changes along the protein chain. The RMSF for residue i is:

$$\text{RMSF}_i = \sqrt{\frac{1}{T} \sum_{t=1}^T (r'_i(t) - r_i(t_{\text{ref}}))^2} \quad (9)$$

In eq. (9), Where T is the trajectory time over which the RMSF is calculated, t_{ref} is the reference time, r_j is the position of residue i , r' is the position of atoms in residue i after superposition on the reference and the angle brackets indicate that the average of the square distance is taken over the selection of atoms in the residue.

2. MATERIALS AND METHODS

A molecular dynamics simulation is an extensively utilized system to appreciate the possessions of the structure and near configuration, interactions occupied molecules.^[22,23] The molecular dynamics simulation is performed by Schrödinger for minimization energy. The molecular dynamic simulation was achieved for the apiece method by employing Desmond. The entire progression is accomplished in three phases for instance system builder, minimization and molecular dynamics.^[17] Solvation creator was utilized to excellent TIP₃P like as solvent model using orthorhombic edge box and charges were neutralized utilized sodium (34Na^+) and chloride (26Cl^-) ions and molecular dynamic simulations consuming time (10,008nsec) bcr-abl/C200-3231 complex. Previously simulation we certified that the method has certainly no steric clashes by exposing it to the progression of energy minimization. The method equilibration was completed through NVT ensemble utilized shake algorithm and via getting the temperature adequate to 300K and the pressure adequate

to 1.01325 bar. After equilibration 10ns molecular dynamic simulation was intended for the bcr-abl/C200-3231 compound complex. The bond length was contrived utilizing the LINCS algorithm the simulations were conceded for 10ns and trajectories were evaluated. Subsequently conclusion of molecular dynamic simulations of the ensuing md.out.cms file was utilized to analyze RMSD of bcr-abl/C200-3231compound complex, ligand RMSF, protein RMSF, protein-ligand interactions and ligand torsion study.^[19,24,25,26,27]

2.1 ESTABLISHMENT OF THE PROTEIN STRUCTURE INTENDED FOR MOLECULAR DYNAMICS SIMULATION

The X-ray configuration of bcr-abl/C200-3231compound was employed starting the Protein Data Bank (PDB: 3CS9). The configuration was a theme for a consignment of creation of zero-orders to metal, disulfide bond, bond orders and hydrogenation. The pH of 7.0 ± 2.0 created appropriate ionization situations for bound inhibitors.^[28] The deletion of undesirable water fragments and optimization of energy was accompanied by maestro expending the OPLS3 dynamism field.^[29] To construct the bcr-abl/C200-3231 compound and the X-ray configuration of the bcr-abl/C200-3231 compound was occupied commencing the PDB for the reason that the Nilotinib compound in 3CS9 is the edifice the most analogous to C200-3231. To construct the bcr-abl/C200-3231 compound 3CS9 was used. We renewed the Nilotinib referent to C200-3231 expending 3D constructor in Maestro (Schrödinger, INC). The configuration was a theme for the consignment of hydrogenation, generation of suitable ionization state, creation of zero-order bonds to metal, H-bond optimization, bond orders, disulfide bonds and confiscating water fragments and enhancing energy through maestro expending the OPLS3 dynamism field.^[29,30]

2.2 PROGRESSION FOR MOLECULAR DYNAMICS SIMULATIONS

A molecular dynamics system format unit was used to establish active structures.^[17] The bcr-abl/C200-3231 compound was occupied in the orthorhombic rectangle box with a buffer expanse of 10Å expending the modest fact charge water pattern. The progression was neutralized by the addition of counter ions and a salt concentration of 0.15 M NaCl.

2.3 MOLECULAR DYNAMICS SIMULATIONS

The molecular dynamics simulation system was assembled by Desmond.^[17] OPLS3 dynamism field was assembled to analyze the interactions concerning entire molecules.^[17,31] The eradicate radius was conventional 9Å intended for the small range electrostatic and Vander Waals collaborations. Preliminary pressure and temperature were conventional 300K

and 1.01325 bar sequentially. The molecular dynamics simulation utilized a time step of 10ns. The procedure of the Desmond file was used for molecular dynamics equilibration and minimization of the methods. As a final point 10ns atomistic molecular dynamics simulations for apiece, bcr-abl/C200-3231 compound system was achieved 4 times via changing the initially composed trajectory structures during the molecular dynamics simulations utilized in the post-standard progression molecular dynamics study.^[17]

2.4 POST-STANDARD PROGRESSION MOLECULAR DYNAMICS STUDY

The trajectory texture achieved from the molecular dynamics simulations was exposed to a post-standard progression molecular dynamics study to quantitatively measure the bcr-abl/C200-3231 compound interactions. The etiquettes employed in the Maestro minor atoms drug innovation were utilized to explain hydrophobic collaborations, salt bridge interactions, hydrogen bonds and π - π assembling.^[19]

2.5 TRAJECTORY ASSEMBLING STUDY

The Desmond trajectory raceming device was utilized to descriptive configurations commencing the simulations. The heavy atom RMSD (root mean square deviation) circumstance was utilized as an essential analogous metric and chiral raceming with average linkage. The RMSD was utilized as the raceming technique. The amalgamated space was customized exist 2.0 Å. The edifice concluded the prevalent number of proximities in the fundamental ancestry was utilized as the illustrative configuration.

3. RESULTS AND DISCUSSION

The bcr-abl/C200-3231 complex was verified to be admirable established in the interactions concerning bcr-abl/C200-3231 complex facts are mentioned in table 1; table 2; table 3 and table 4 and the following analyzes were conducted based on this structure.^[18]

Table 1: Docking score, binding energy and possible interactions of top Indolizine analogue C200-3231.

Compound	Dock score	Binding energy (kcal/mol)	Interactions
Nilotinib (reference molecule)	-17.812	-144.921	H ₂ O, GLU286, THR315, PHE382, TYR253, ASP381, MET318
C200-3231	-11.596	-99.264	TYR253, PHE382, ASP381, H ₂ O, ALA269, ILE293, LEU248, MET290

Table 2: The Absorption Distribution Metabolism Excretion parameter & drug characteristic of Indolizine analogue C200-3231.

Principal descriptor	Nilotinib	C200-3231	Standard limits
Metab	1	4	1-8
MW	307.363	397.473	130.0-725.0
SASA	593.278	736.11	300.0-1000.0
DonorHB	1	0	0.0-6.0
AcceptorHB	4.5	4	2.0-20.0
QPlogS	-4.545	-7.258	-6.5-0.5
QPlogHERG	-5.729	-6.986	Concern below -5
QPPCaco	1327.79	2117.105	<25 poor >500 great
QPlogBB	0.566	-0.496	-3.0-1.2
QPPMDCK	672.107	1112.856	<25 poor >500 great
QPlogKp	-1.749	-0.844	-8.0- -1.0
QPlogKhsa	0.378	1.151	-1.5-1.5
%HOA	100	100	>80% is high <25% is poor
PSA	68.332	57.811	7.0-200.0
Rule of five	0	1	Mol. wt.<500 QPlogP o/w<5 Donor HB≤5 acceptorHB≤10
Rule of three	0	1	Maximum 3

Table 3: The structure of Nilotinib (referencing molecules) and five Indolizine analogue C200-3231.

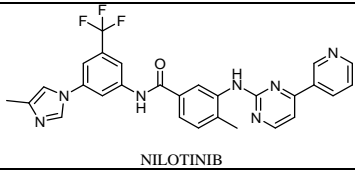
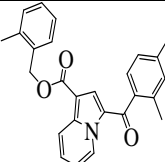
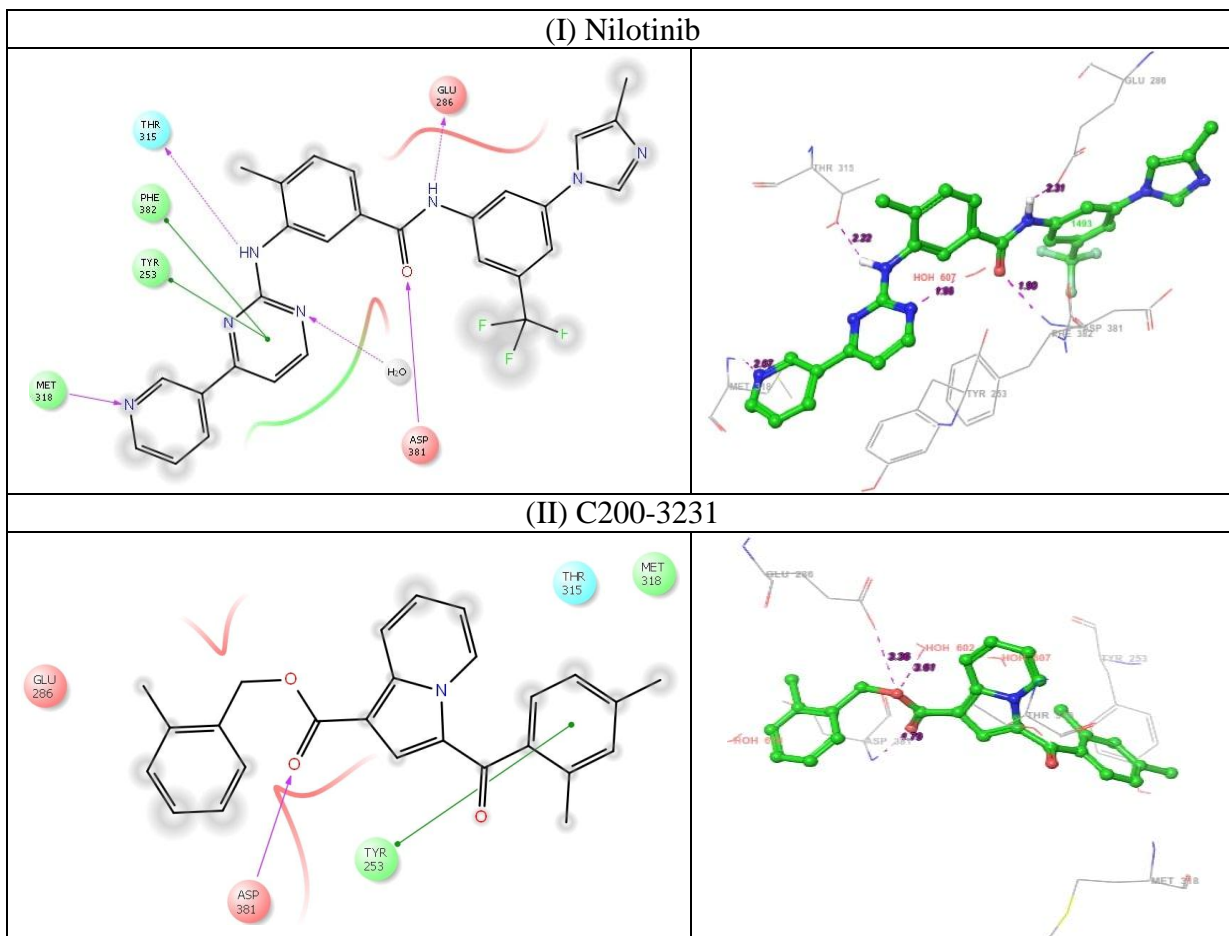
Nilotinib	 <p>NILOTINIB</p>
C200-3231	

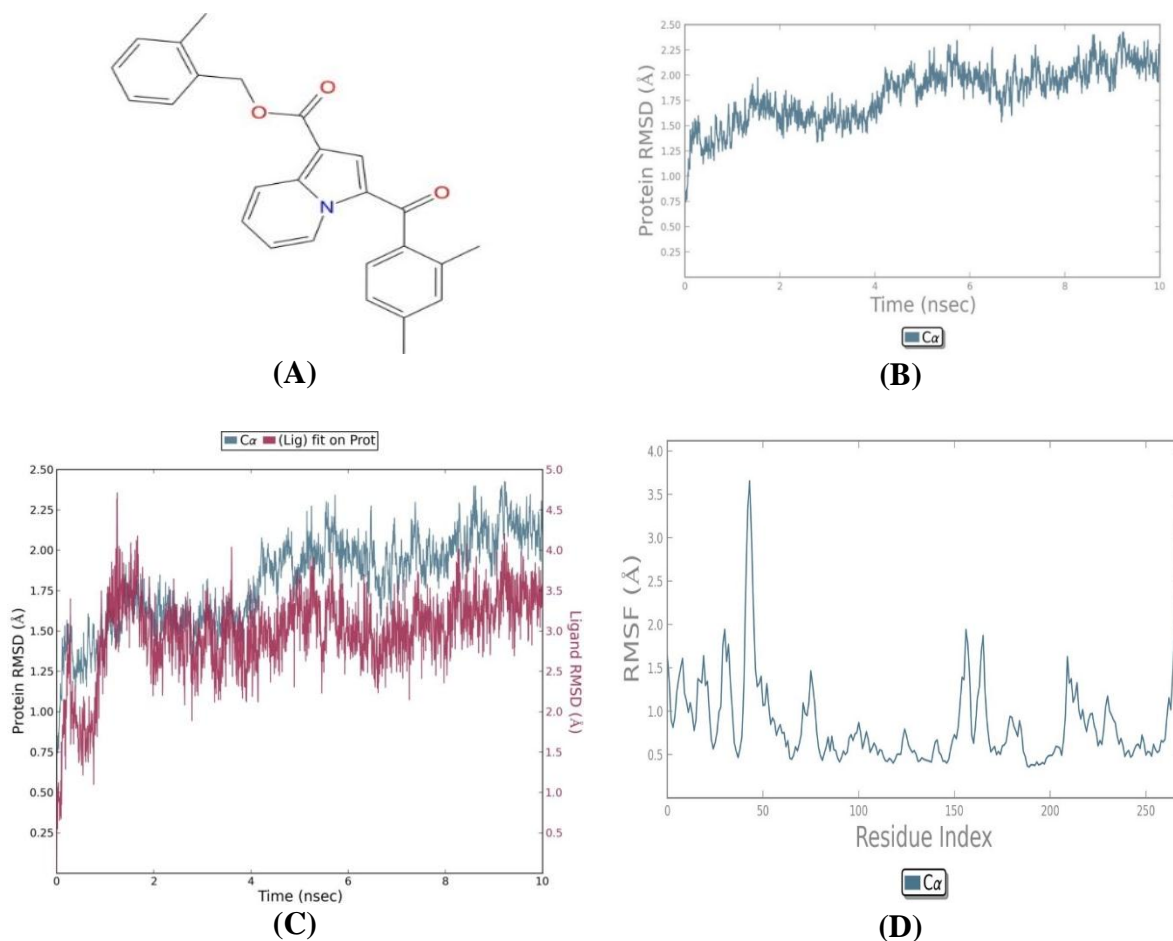
Table 4: 2D and 3D structures of Protein-ligand complex interactions (I) Nilotinib with bcr-abl Protein (II) C200-3231 with bcr-abl Protein.

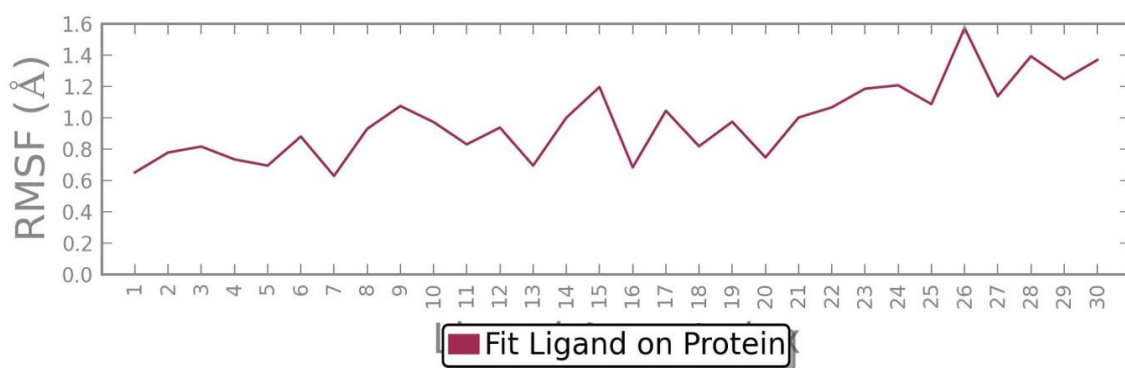


3.1 STRUCTURAL STRENGTH AND STABILITY ANALYSIS

A root means square deviation (RMSD) standard of heavy atoms mentioned through the preliminary structure was intended for the bcr-abl/C200-3231 complex. The bcr-abl/C200-3231 complex RMSD was utilized to measure the ordinary changes in the movement of a selected atom for a specific edge with details to a reference edge. The bcr-abl/C200-3231 complex RMSD was calculated for all frames in the trajectory.^[31] The bcr-abl/C200-3231 complex RMSD was displayed of the bcr-abl/C200-3231 complex provided structural conformation by the simulation (Figure 1C). The bcr-abl/C200-3231 complex root means square fluctuation (RMSF) regarding the finale of the simulation was about specific thermal ordinary structures. The RMSF was convenient and intended for illustrating confined modifications of the protein chain. The bcr-abl/C200-3231 complex RMSF peaks specify regions of the protein fluctuation the greatest through the simulation. The C200-3231 RMSF was convenient and intended for illustrating modifications in the C200-3231 sites. The C200-3231 RMSF is related to the bcr-abl protein and its entropic role in the binding result (Figure

1E). The acceptable C200-3231 on the bcr-abl protein complex was the major affiliated backbone and RMSF was dignified on the heavy atoms (Figure 1D). The time development of root mean square deviation for complex in the course of 10ns molecular dynamic simulations is displayed in (Figure 1B; 1C). The root means square deviation of all simulation methods advanced steady standards values in the last 5ns. This specified that the bcr-abl/C200-3231 complex had equilibrated facilitating the next study. The highest conventional RMSD significance for the bcr-abl/C200-3231 complex was the experimental range from 1 to 2.50 Å. This is a reason for the N-terminal and C-terminal displayed great fluctuation (Figure 1D). The bcr-abl/C200-3231 complex RMSD exploration indicated if the simulation had equilibrated. The bcr-abl/C200-3231 complex was the greatest firm stable complex.



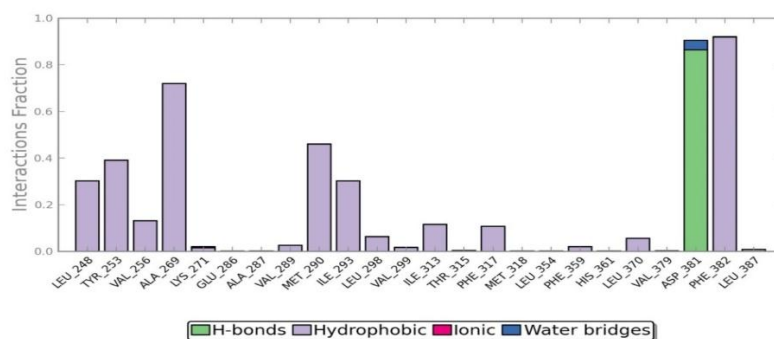


(E)

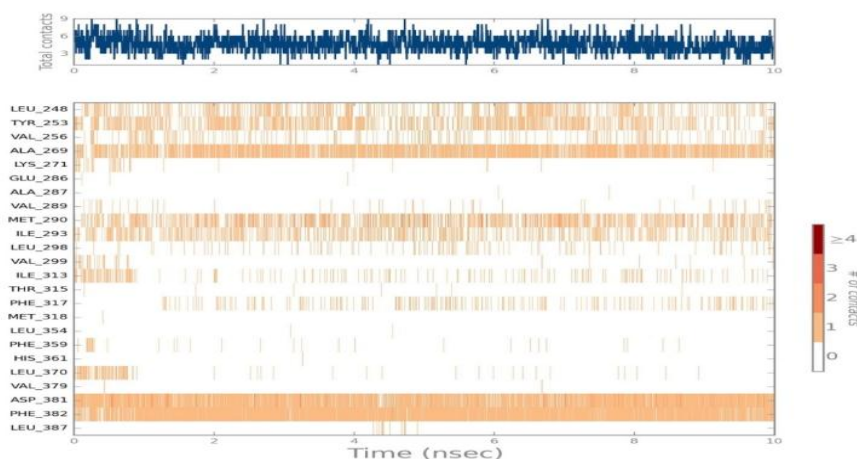
Figure 1: (A-E) RMSD and RMSF showing with protein-ligand complex (bcr-abl/C200-3231) pattern (A) 2D structure of ligand (C200-3231). (B) RMSD of bcr-abl protein (2.50Å). (C) RMSD of bcr-abl/C200-3231 complex (4.5Å). (D) RMSF of bcr-abl protein (3.5Å). (E) Root Mean Square Fluctuation of bcr-abl/C200-3231 complex up to 1.6 Å.

3.2 BCR-ABL/C200-3231 COMPLEX INTERACTION STUDY

The interactions analysis was carried out for bcr-abl/C200-3231 complex. The bcr-abl/C200-3231 complex was characterized by hydrophobic bond, hydrogen bond, water bridges and ionic. There were 24 residues interacted with a value of 0.3 that 70% of the simulation time the specific interaction is sustained (Figure 2A). C200-3231 compound was having a -11.596 kcal/mol dock score and MMGBSA bind energy -99.264 kcal/mol mentioned in Table 1. ASP381 attached oxygen atom with hydrogen bond of the Indolizine around A pocket. Bcr-abl/C200-3231 complex suggest the 86% contacts (Figure 2B). ASP381 formed water bridges. PHE382, ALA269, ILE293, LEU248, MET290 and TYR253 formed a hydrophobic interaction with phenyl around the A pocket. TYR253 interacted with π - π lipophilic interaction.



(A)



(B)

Figure 2: Protein-ligand interaction throughout the simulation study for C200-3231. The bcr-abl/C200-3231 complex contacts are characterized into four categories: hydrogen bonds, and hydrophobic, ionic, and water-bridged interactions (A). Values over 1.0 are assured protein residue for the summary of contacts more than 0.3 perhaps making multiple contacts with bcr-abl/C200-3231 complex (B).

Dial plots explained the conformation of the torsion completed the simulation progression of 10nsec. The preliminary simulation progression was the focus of the dial plot and the expansion of time was plotted radially exterior. The possible density of the torsion arranged in the bar plots was deliberated by the data arranged on the dial plots. There were six rotational bonds contemporary in the C200-3231. The standards of probable for torsional bonds were arranged on the left Y-axis of the graph formal ranges from 0.00 to 1.34, 0.00 to 3.41, 0.00 to 6.46, 0.00 to 8.06, 0.00 to 8.15, 0.00 to 13.10 kcal/mol. The histogram (bar plots) and torsion potential affiliations of the ligand C200-3231 completed the development of the molecular dynamic simulation trajectory. The C200-3231 compound concluded that undertaken conformational action nourishes a bcr-abl/C200-3231 conformation. Ensuing possessions were studied to explain the strength and stability of the C200-3231 in the binding domain of bcr-abl protein receptors in the simulation of 10nsec as shown in (Figure 3C).

1. rGyr (radius of gyration) – The radius of gyration was explored to enlarge the C200-3231.
2. MolSA (molecular surface area) – The molecular surface area having 1.4 Å studied for radius, this value was corresponding to Vander Waals surface area.
3. SASA (solvent accessible surface area) – The surface area of a C200-3231 is easy to get to water molecules.

4. PAS (polar surface area) – The solvent-accessible surface area in a C200-3231 subscribed simply using oxygen and nitrogen molecules.

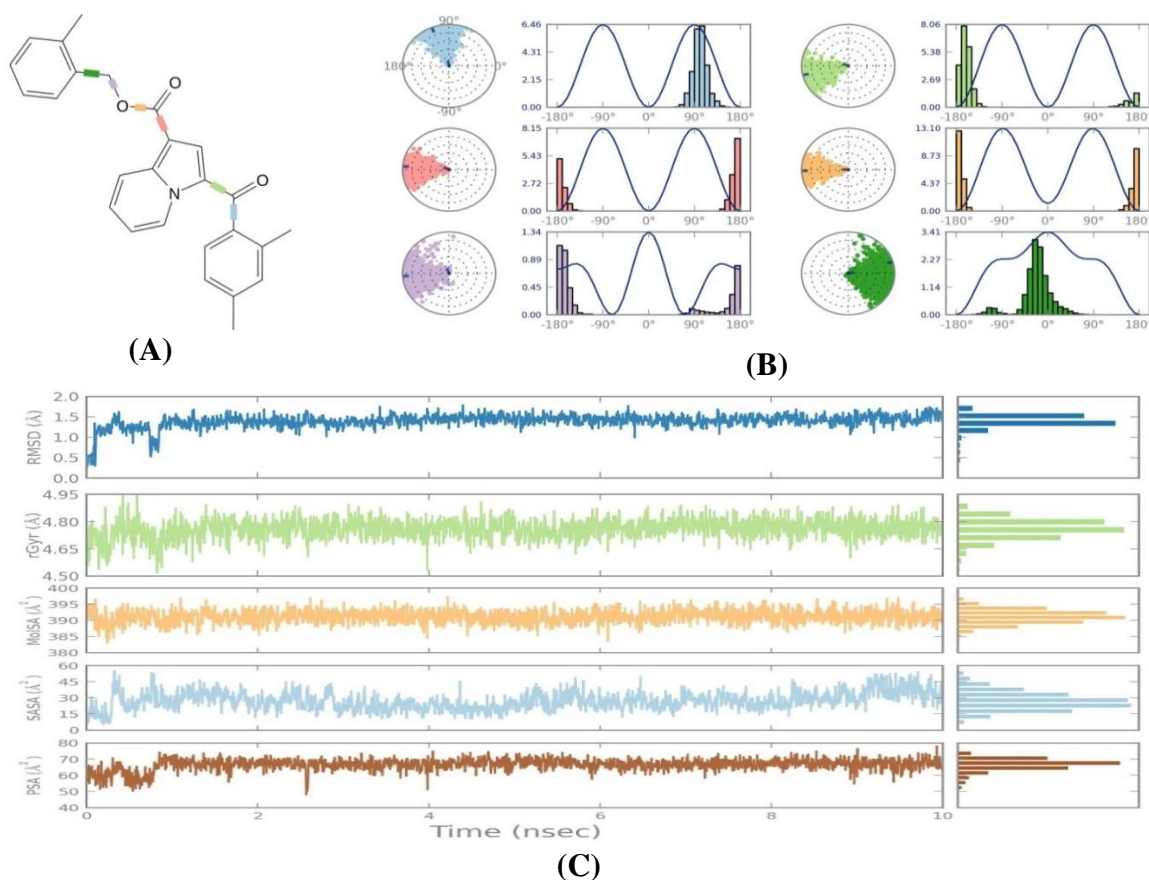
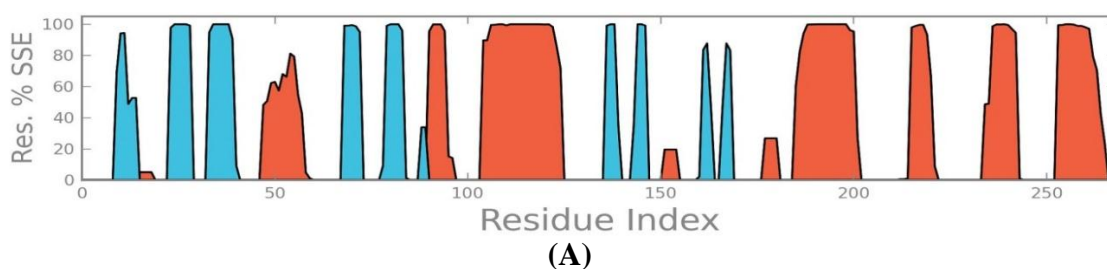
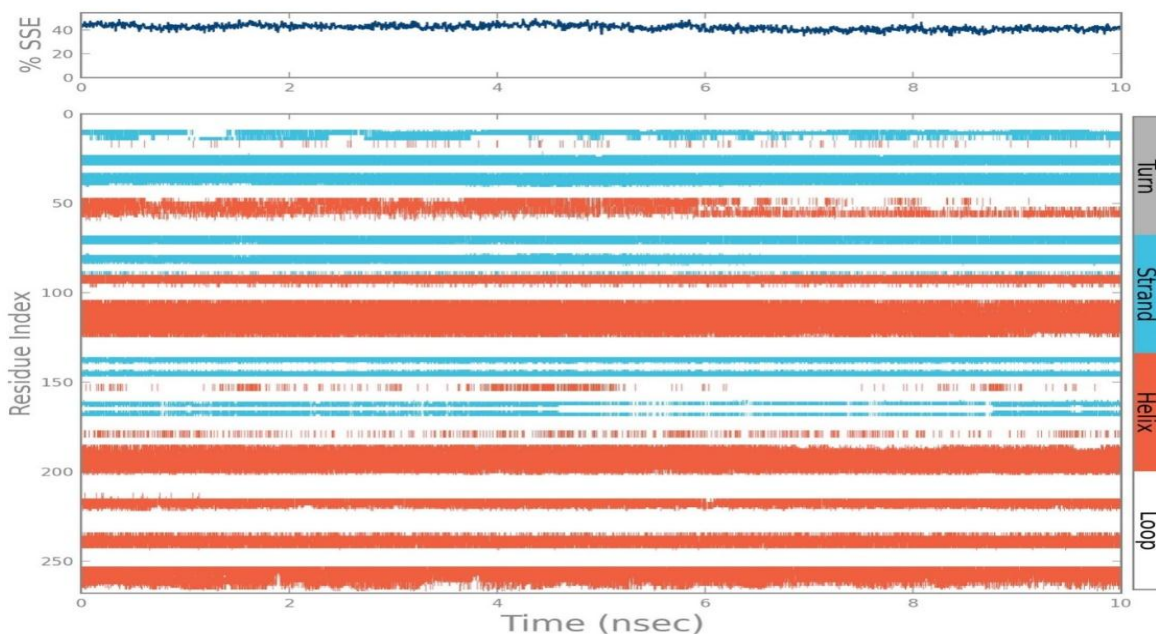


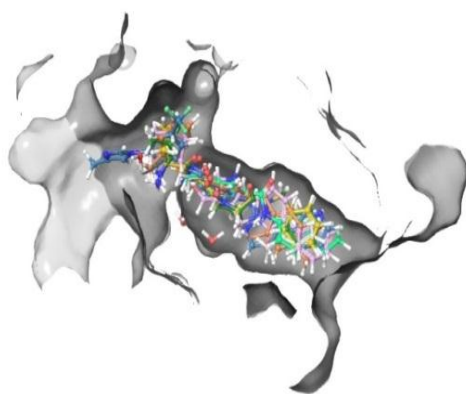
Figure 3: The 2D schematic of a ligand with colour-coded rotatable bonds is shown in (A). Torsion profile of C200-3231 during simulations trajectory of 10nsec has shown (B). The torsion variation in the C200-3231 properties during 10nsec simulations has been shown (C). The ligand C200-3231 torsion portrait (Figure 3; A, B, C) was designed to find the conformational variations of each rotatable bond in the compound C200-3231 through the progression of the simulation path (0.00 to 10.00nsec). The colour-coded rotatable bonds display the 2D schematic diagram of C200-3231 (Figure 3A). Respectively rotatable bond torsion was conveyed using a dial plot and bar plots of a similar colour (Figure 3B).



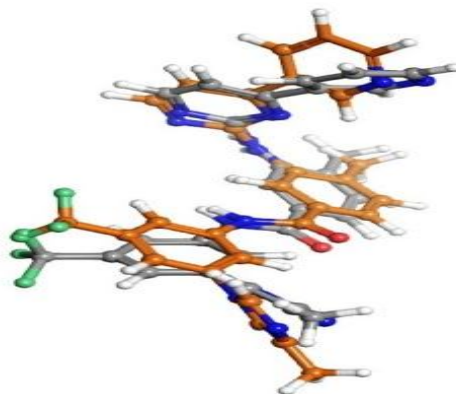


(B)

Figure 4: The protein secondary structure elements (SSE) (42.29%) similar to alpha helices (27.83%) and beta-strands (14.45%) were examined during simulation (A). The strategy reports secondary structure elements scattering through residue index using the protein structure. The strategy précises the protein secondary structure elements configuration and conformations for every trajectory edge concluded the progression of the simulation. The strategy monitored every residue and the protein secondary structure elements obligate concluded time (B).



(A)



(B)

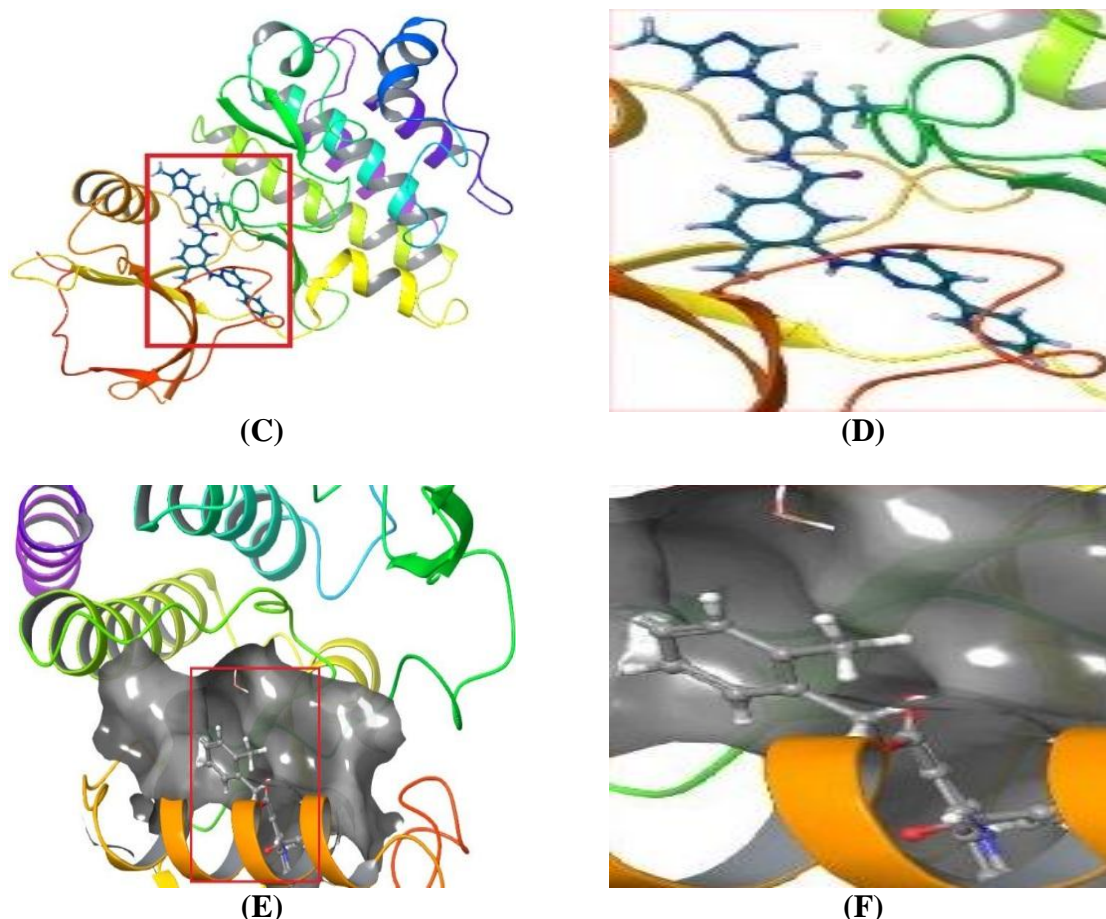


Figure 5: (A) Shows the surface view of the electrostatic potential for tyrosine kinase domain overlapping docked conformation of Nilotinib (mustard yellow), C200-3231 (grey), CHEMBL1196530 (pink), CHEMBL1188037 (yellow), CHEMBI101411 (blue), G133-0631 (orange). (B) Shows the molecular docking validation for referencing molecules Nilotinib and molecule C200-3231 utilized optimized parameters. The docked pose of C200-3231 (grey colour) overlapped with the Nilotinib (orange colour) shown in B. (C) Shows the binding mode of Nilotinib (blue) on tyrosine kinase dimer of bcr-abl protein at the interface of chain A pocket (PDB 3CS9). The Nilotinib is shown in stick with blue colour, red, blue and white colour for the oxygen, nitrogen and hydrogen, respectively. (D) Shows the square box in panel C is an enlarged close-up view of the contact potential of chain A at the interface bcr-abl binding pocket of the tyrosine kinase dimer. (E) Shows the binding mode of C200-3231 (grey) on tyrosine kinase dimer of bcr-abl protein at the interface of chain A pocket (PDB 3CS9). The C200-3231 is shown in stick with grey colour, red, blue and white colour for the oxygen, nitrogen and hydrogen, respectively. (F) Shows the square box in panel E is an enlarged close-up view of the contact potential of chain A at the interface bcr-abl the binding pocket of the

tyrosine kinase dimer. Here the Nilotinib and C200-3231 share a common binding pocket at the interface of a dimer.

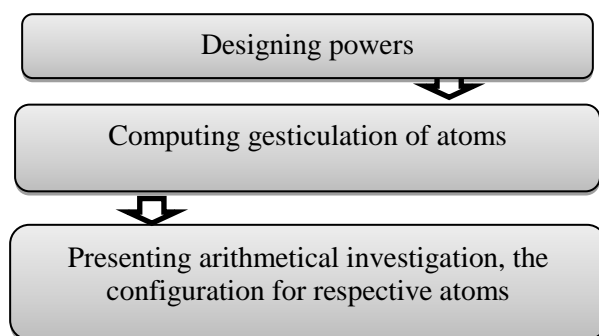


Figure 6: The molecular dynamics simulation progression flowchart.

In the world subcontinent, the cure preference is strongly influenced by Bosutinib, Nilotinib, Dasatinib, Ponatinib, Bafetinib and Imatinib in the management of chronic myeloid leukaemia.^[1,3,15,32] All these medicines are expensive and need to prolong the period of cure allied with conflict to proliferative growth of granulocyte stem cells.^[2] Nilotinib and Imatinib have exposed moral efficacy and minor toxicity but its great cost and possibly argue with the chromosomal abnormality and precise cytogenetic abnormalities however a steady property of leukaemia cells in chronic myeloid leukaemia but engage in no character in the pathogenesis of leukaemia cells.^[1,15,3,33] The chromosome was eradicated commencing their marrow and metaphases displaying the Philadelphia chromosome abnormalities continued.^[15,22] Indolizine is a vital anticancer drug in Indian customs for approximate 2,000 years.^[18] The Indolizine nucleus is undertaking extensive exploration for its anticancer potential with the innovation of Camptothecin.^[34] Indolizine moiety has exposed an extensive series of activity delight herbicidal, ACE inhibitors, antihistaminic, antimicrobials, anticancer, phosphatase inhibitors, phosphodiesterase inhibitors, antioxidants, anti-inflammatory, antitubercular, aromatase inhibitors, uterotrophic activity, antileishmanic.^[32] An Indolizine derivative has exposed inhibition influence resistance tyrosine kinase, Philadelphia chromosome oncogene, and bcr-abl oncoprotein.^[34] Numerous innate compounds and their chemically amalgamated products have revealed tyrosine kinase inhibitors and hindering Philadelphia chromosome oncogenes by targeting CML.^[17] C200-3231 is one of the revealed strong resistances against the Philadelphia chromosome oncogene.^[17] Indolizine is a cost-effective usual product against tyrosine kinase inhibition at precise a amount concentration and has natural compounds to resist side effects for the duration of medicament.^[30] Using curtailed revealed factors and parameters. We have

selected Indolizine analogues against tyrosine kinase to prove their inhibitory action to against the Philadelphia chromosome oncogene, a tyrosine kinase inhibitor, bcr-abl oncoprotein.^[18] The current research is dedicated to molecular dynamics simulation exploration to discover novel tyrosine kinase inhibitors. Virtual screening was utilized to evaluate the interaction of C200-3231 in the bcr-abl binding pocket A to focused enzyme creates in docking score. Greater the negative significance of the docking score (-11.596 kcal/mol) has revealed the strength and stability of the relationship of the tyrosine kinase inhibitor.^[18] We calculated the virtual binding affinity of 2,154 Indolizine analogues binding with tyrosine kinase enzyme of BCR-ABL protein pocket A. The calculation of binding affinity was agreed by molecular docking methodology in two docking methods, standard precision (SP) (50%) to conclude was finished by extra precision (XP) (20%) of docking for C200-3231. Furthermore, estimating the similarities for Nilotinib for exploratory validation protocol and Indolizine analogues the greatest interacting ligand was C200-3231 having a docking score of -11.596 kcal/mol. Indolizine analogues the greatest interacting ligand C200-3231 was using docking score (-11.596 kcal/mol), MM-GSA Dg bind (-99.264 kcal/mol), best interactions and ADME for that reason certify the qualified binding energy for bcr-abl/C200-3231 table 1; table 2; table 3 and table 4.^[27] The consequences of docking design using Glide_{v6.9} to discover the binding site of C200-3231 accompanying reference ligand (Nilotinib) on tyrosine kinase dimer exposes C200-3231 competitive bind at the edge of pocket A of the tyrosine kinase dimer. C200-3231 has revealed lower binding energy (-99.264kcal/mol) in contrast to Nilotinib (-144.921). But the interaction for C200-3231 (TYR253, PHE382, ASP381, H₂O, ALA269, ILE293, LEU248, and MET290) was higher than Nilotinib (H₂O, GLU286, THR315, PHE382, TYR253, ASP381, and MET318) (Table 1; Table 4). Consequently, these interactions with C200-3231 ligand strength swapping the dynamic establish an arrangement of tyrosine kinase dimer. The electrostatics possible designs concluded tyrosine kinase dimer using Indolizine docked conformation and configuration displays that C200-3231 ligand segments the similar binding site. The molecular dynamics simulations of C200-3231 revealed the all-embracing stability of the bcr-abl/C200-3231 complex. The radius of gyration and molecular surface area explicit for the C200-3231 residues are constant for the duration of the whole simulation progression. The radius of gyration differences for C200-3231 in the receptor-binding domain of the bcr-abl protein receptor was intended to be analogous which fluctuates stuck between 3.44 and 3.65 Å (Figure 1D) and argues the secure activities of the C200-3231 done the perfect simulation trajectory. The solvent-accessible surface area and polar surface area for the C200-3231

occur fluctuation in the diagram till 10nsec but subsequently, these features virtually steady expose the stability of the ligand binding in the receptor domain accomplishing the simulation trajectory. The all-embracing RMSF below 2.0Å (Figure 1E) intended for C200-323 specifies the stability of the compound to be calculated accompanying in-vitro and in-vivo Philadelphia chromosome oncogene inhibition. Consequently, screened superior performance of C200-3231 (Indolizine ring containing moiety) on entirely parameters specifically ligand construct molecular docking, MM-GBSA, ADME properties (QikProp possessions) (Figure 5; A; B; E; F)^[17] and molecular dynamics reveals C200-3231 compound may be dynamic resist Chronic Myeloid Leukemia.

4. CONCLUSION

Appreciating bcr-abl/C200-3231 interactions is significant for scheming purpose selective inhibitors. In this analysis, we petitioned genuine methodology that amalgamated molecular modelling and molecular dynamics simulation to develop the contemporary appreciation of the judicious of C200-3231 for bcr-abl inhibitors. According to this analysis established that the hydrogen bond concerning ASP381 of bcr-abl protein. The Indolizine of C200-3231 was a vital interaction as specified through the interaction study. In the MM-GBSA study and we recommend that substitution of pyrimidine, pyridine and imidazole with Indolizine can rise judicious for bcr-abl inhibitors. According to this analysis proposes such as the secondary structure of the amendable alpha helix (27.83%), clarifying of beta-strand (14.45%) and contact with TYR253, PHE382, ASP381, H₂O, ALA269, ILE293, LEU248, and MET290 to binding site establish was vital. These residues designed a π - π interaction using the bcr-abl protein selective inhibitor. Devoid of X-ray edifices is problematic to associate interactions concerning bcr-abl/C200-3231 complexes of importance. The bcr-abl/C200-3231 complex-forming is useful in this analysis at slight facilitates the relationship of interactions. But the situations make not clarify the selectivity. Using coalescing molecular dynamics simulation, clustering study and stable interactions study concerning protein and inhibitor may perhaps explain. For that, the reason of molecular dynamics simulation is a potent and dominant implement for explaining the dynamics of bcr-abl/C200-3231 interactions and to maintenance drug design. The perceptions achieved commencing the molecular dynamic simulations may perhaps be valuable for scheming novel selective bcr-abl inhibitors.

5. ACKNOWLEDGEMENTS

Indian Institute of Information Technology Allahabad is thankful for providing Schrodinger, Desmond and ADME predictor facilities. SU is thankful to IFTM University Moradabad for doctor of philosophy guidance. J is thankful to the Department of Information technology for being an innovative researcher.

6. CONFLICTS OF INTEREST

The authors have declared no competing interests.

7. REFERENCES

1. Jabbour, E., El Ahdab, S., Cortes, J. and Kantarjian, H., 2008. Nilotinib: a novel Bcr-Abl tyrosine kinase inhibitor for the treatment of leukaemias. *Expert Opinion on Investigational Drugs*, 17(7): 1127-1136.
2. Bedi, A., Zehnbauser, B., Barber, J., Sharkis, S. and Jones, R., 1994. Inhibition of apoptosis by BCR-ABL in chronic myeloid leukaemia. *Blood*, 83(8): 2038-2044.
3. Kumar, H., Raj, U., Gupta, S. and Varadwaj, P., 2016. In-silico identification of inhibitors against mutated BCR-ABL protein of chronic myeloid leukaemia: a virtual screening and molecular dynamics simulation study. *Journal of Biomolecular Structure and Dynamics*, 34(10): 2171-2183.
4. Baccarani, M. and Dreyling, M., 2010. Chronic myeloid leukaemia: ESMO Clinical Practice Guidelines for diagnosis, treatment and follow-up. *Annals of Oncology*, 21: v165-v167.
5. Zhou, F., Jin, R., Hu, Y. and Mei, H., 2017. A novel BCR-ABL1 fusion gene with genetic heterogeneity indicates a good prognosis in a chronic myeloid leukaemia case. *Molecular Cytogenetics*, 10 (1).
6. Kralovics, R., Passamonti, F., Buser, A., Teo, S., Tiedt, R., Passweg, J., Tichelli, A., Cazzola, M. and Skoda, R., 2005. A Gain-of-Function Mutation of JAK2 in Myeloproliferative Disorders. *New England Journal of Medicine*, 352(17): 1779-1790.
7. Mir, R. and AbuDuhier, F., 2016. Rapid detection of JAK2 V617F mutation in myeloproliferative disorders. *Annals of Oncology*, 27: vii79.
8. Pane, F., Frigeri, F., Sindona, M., Luciano, L., Ferrara, F., Cimino, R., Meloni, G., Saglio, G., Salvatore, F. and Rotoli, B., 1996. Neutrophilic-chronic myeloid leukaemia: a distinct disease with a specific molecular marker (BCR/ABL with C3/A2 junction) [see comments]. *Blood*, 88(7): 2410-2414.

9. Shan, Y., Seeliger, M., Eastwood, M., Frank, F., Xu, H., Jensen, M., Dror, R., Kuriyan, J. and Shaw, D., 2008. A conserved protonation-dependent switch controls drug binding in the Abl kinase. *Proceedings of the National Academy of Sciences*, 106(1): 139-144.
10. Rossari, F., Minutolo, F. and Orciuolo, E., 2018. Past, present, and future of Bcr-Abl inhibitors: from chemical development to clinical efficacy. *Journal of Hematology & Oncology*, 11(1).
11. Soverini, S., Abruzzese, E., Bocchia, M., Bonifacio, M., Galimberti, S., Gozzini, A., Iurlo, A., Luciano, L., Pregno, P., Rosti, G., Saglio, G., Stagno, F., Tiribelli, M., Vigneri, P., Barosi, G. and Breccia, M., 2019. Next-generation sequencing for BCR-ABL1 kinase domain mutation testing in patients with chronic myeloid leukemia: a position paper. *Journal of Hematology & Oncology*, 12(1).
12. Goldman, J. and Melo, J., 2008. BCR-ABL in Chronic Myelogenous Leukemia – How Does It Work? *Acta Haematologica*, 119(4): 212-217.
13. Peng, H., Huang, N., Qi, J., Xie, P., Xu, C., Wang, J. and Yang, C., 2003. Identification of novel inhibitors of BCR-ABL tyrosine kinase via virtual screening. *Bioorganic & Medicinal Chemistry Letters*, 13(21): 3693-3699.
14. García-Gutiérrez, V. and Hernández-Boluda, J., 2020. Current Treatment Options for Chronic Myeloid Leukemia Patients Failing Second-Generation Tyrosine Kinase Inhibitors. *Journal of Clinical Medicine*, 9(7): 2251.
15. Preisinger, C., Schwarz, J., Bleijerveld, O., Corradini, E., Müller, P., Anderson, K., Kolch, W., Scholten, A. and Heck, A., 2012. Imatinib-dependent tyrosine phosphorylation profiling of Bcr-Abl positive chronic myeloid leukaemia cells. *Leukaemia*, 27(3): 743-746.
16. Nakano, A., Kalia, R. and Vashishta, P., 1999. Scalable molecular dynamics, visualization, and data management algorithms for materials simulations. *Computing in Science & Engineering*, 1(5): 39-47.
17. Shaw, D., 2013. Millisecond-Long Molecular Dynamics Simulations of Proteins on a Special-Purpose Machine. *Biophysical Journal*, 104(2): 45a.
18. Mahaur, S., and S. Upadhyay. 2021. Indolizine: In-Silico Identification of Inhibitors Against Mutated BCR-ABL Protein of Chronic Myeloid Leukemia. *Research Journal of Pharmacology*, ISSN. 2321-5836.
19. Malik, R., Bunkar, D., Choudhary, B., Srivastava, S., Mehta, P. and Sharma, M., 2016. High throughput virtual screening and in silico ADMET analysis for rapid and efficient

- identification of potential PAP248-286 aggregation inhibitors as anti-HIV agents. *Journal of Molecular Structure*, 1122: 239-246.
20. Noe, F. and Tkatchenko, A., 2020. Machine learning for molecular simulation. The annual review of physical chemistry, 71: 16.1-16.30.
21. Boselt, L. and Thurlemann, M., 2021. Machine learning in QM/MM molecular dynamics simulations of Condensed-Phase systems. *Journal of Chemical Theory and Computation*, 17: 2641-2658.
22. Dubey, K. and Ojha, R., 2011. Conformational flexibility and binding energy profile of c-Abl tyrosine kinase complexed with Imatinib: an insight from MD study. *Molecular Simulation*, 37(14): 1151-1163.
23. Pandey, R., Kumbhar, B., Srivastava, S., Malik, R., Sundar, S., Kunwar, A. and Prajapati, V., 2016. Febrifugine analogues as Leishmania donovani trypanothione reductase inhibitors: binding energy analysis assisted by molecular docking, ADMET and molecular dynamics simulation. *Journal of Biomolecular Structure and Dynamics*, 35(1): 141-158.
24. Nakano, A., Kalia, R. and Vashishta, P., 1999. Scalable molecular dynamics, visualization, and data management algorithms for materials simulations. *Computing in Science & Engineering*, 1(5): 39-47.
25. Pandey, R., A. Narula, M. Naskar, S. Srivastava, P. Verma, R. Malik, P. Shah, and V. Prajapati. 2016. Exploring Dual Inhibitory Role of Febrifugine Analogues Against Plasmodium Utilizing Structure-Based Virtual Screening and Molecular Dynamic Simulation. *Journal of Biomolecular Structure and Dynamics* 35, no. 4: 791-804. Informa UK Limited.
26. Pandey, R., Kumbhar, B., Srivastava, S., Malik, R., Sundar, S., Kunwar, A. and Prajapati, V., 2016. Febrifugine analogues as Leishmania donovani trypanothione reductase inhibitors: binding energy analysis assisted by molecular docking, ADMET and molecular dynamics simulation. *Journal of Biomolecular Structure and Dynamics*, 35(1): 141-158.
27. Priya Doss, C., Chakraborty, C., Chen, L. and Zhu, H., 2014. Integrating in Silico Prediction Methods, Molecular Docking, and Molecular Dynamics Simulation to Predict the Impact of ALK Missense Mutations in Structural Perspective. *BioMed Research International*, 2014; 1-14.
28. Shelley, J., A. Cholleti, L. Frye, J. Greenwood, M. Timlin, and M. Uchimaya. 2007. Epik: A Software Program for Pk a Prediction and Protonation State Generation for Drug-Like

- Molecules. *Journal of Computer-Aided Molecular Design* 21, no. 12: 681-691. Springer Science and Business Media LLC.
29. Oltersdorf, T., S. Elmore, A. Shoemaker, R. Armstrong, D. Augeri, B. Belli, and M. Bruncko et al. 2005. An Inhibitor of Bcl-2 Family Proteins Induces Regression of Solid Tumours. *Nature* 435, no. 7042: 677-681. Springer Science and Business Media LLC.
30. Shiv kumar, D., Williams, J., Wu, Y., Damm, W., Shelley, J. and Sherman, W., 2010. Prediction of Absolute Solvation Free Energies using Molecular Dynamics Free Energy Perturbation and the OPLS Force Field. *Journal of Chemical Theory and Computation*, 6(5): 1509-1519.
31. Harder, E., W. Damm, J. Maple, C. Wu, M. Reboul, J. Xiang, and L. Wang et al. 2015. OPLS3: A Force Field Providing Broad Coverage of Drug-Like Small Molecules and Proteins. *Journal of Chemical Theory and Computation* 12, no. 1: 281-296. American Chemical Society (ACS).
32. Weisberg, E., Manley, P., Mestan, J., Cowan-Jacob, S., Ray, A. and Griffin, J., 2019. Correction: AMN107 (nilotinib): a novel and selective inhibitor of BCR-ABL. *British Journal of Cancer*, 121(3): 282-282.
33. Fabarius, A., Giehl, M., Frank, O., Spiess, B., Zheng, C., Müller, M., Weiss, C., Duesberg, P., Hehlmann, R., Hochhaus, A. and Seifarth, W., 2007. Centrosome aberrations after nilotinib and imatinib treatment in vitro are associated with mitotic spindle defects and genetic instability. *British Journal of Haematology*, 138(3): 369-373.
34. Wall, M., M. Wani, C. Cook, K. Palmer, A. McPhail, and G. Sim. 1966. Plant Antitumor Agents. I. The Isolation and Structure of Camptothecin, A Novel Alkaloidal Leukemia and Tumor Inhibitor from *Camptotheca Acuminata*^{1,2}. *Journal of The American Chemical Society* 88, no. 16: 3888-3890. American Chemical Society (ACS).